ELSEVIER

Journal of Power Sources 54 (1995) 58–62

JOURNAL OF POWER SOURCES

Thin-film rechargeable lithium batteries *

J.B. Bates, N.J. Dudney, D.C. Lubben, G.R. Gruzalski, B.S. Kwak, Xiaohua Yu, R.A. Zuhr

Solid State Division, Oak Ridge National Laboratory, Oak Ridge, TN 37831-6030, USA

Abstract

Thin-film rechargeable batteries with a lithium metal anode, an amorphous inorganic electrolyte, and cathodes of amorphous V_2O_5 and crystalline and amorphous $Li_xMn_2O_4$ have been fabricated and characterized. The performance of the thin-film cells was evaluated at different current densities and, in the case of Li–V_2O_5, at several temperatures. Electrical measurements show that the current density of the thin-film cells is limited by the lithium-ion mobility in the cathodes. The resistance of Li–$Li_xMn_2O_4$ cells with crystalline cathodes is about two orders of magnitude lower than that of Li–V_2O_5 cells with amorphous cathodes.

Keywords: Rechargeable lithium batteries; Thin-film batteries

---

1. Introduction

Thin-film lithium batteries based on lithium metal anodes and cathodes of oxide lithium intercalation compounds including V_2O_5 and $Li_xMn_2O_4$ have been under investigation in this laboratory for several years. The development of these cells was made possible by the unique amorphous inorganic electrolyte, lithium phosphorus oxynitride, that we have described previously [1]. Recently, a multilayer protective coating was developed so that cells can be operated in air. In this paper, we discuss the cycle behavior and rate capability of Li–V_2O_5 cells at different temperatures and present some recent results on Li–$LiMn_2O_4$ cells with cathodes that were deposited by evaporation and sputtering.

2. Experimental procedures

A cross-sectional drawing of a typical thin-film battery is shown in Fig. 1, and the fabrication steps are illustrated in Fig. 2. The sputtering steps were carried out using 2 in. magnetrons operating in either a d.c. or r.f. mode with a target to substrate distance of 5 cm. The batteries were fabricated onto 25 mm × 25 mm substrates prepared with 2000-Å-thick current collectors deposited by sputtering. For V_2O_5, the substrates included glass microscope slides and Coors' ADS 996 alumina, and the current collectors were V. For the $Li_xMn_2O_4$ cells, the substrates were alumina and the current collectors were either V or Pt depending on whether a post deposition anneal of the cathode was made. The cathodes measured 11 mm × 11 mm and were 0.13 to about 1 μm thick.

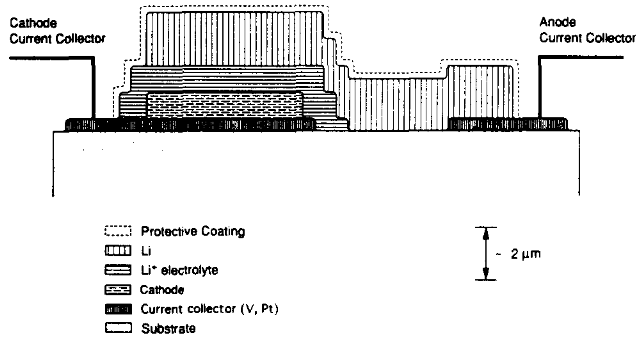

Fig. 1. Schematic cross section of a thin-film lithium battery.

Most of our investigations of thin-film cells have been made using V_2O_5 cathodes. The phase and microstructure of the films are sensitive to several process variables including substrate temperature, substrate bias, and

---

* The article has been authored by a contractor of the US Government under contract No. DE-AC05-84OR21400. Accordingly, the US Government retains a nonexclusive, royalty-free license to publish or reproduce the published form of this contribution, or allow others to do so, for U.S. Government purposes.

Elsevier Science S.A.
SSDI 0378-7753(94)02040-A

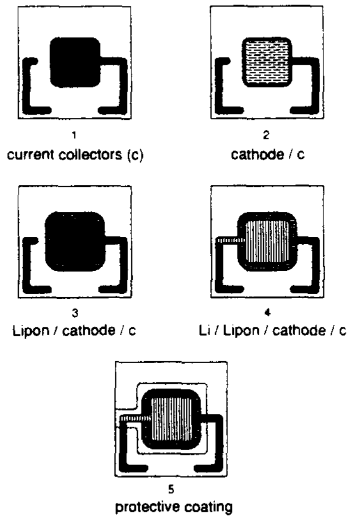

Fig. 2. Layer geometry and fabrication steps.

process gas composition. The form we have found best suited for thin-film batteries is deposited at ambient temperature by d.c. sputtering of V targets in 20 mtorr of an Ar + 14% O_2 gas mixture and with a substrate bias between -5 and -10 V. Although the charge/discharge curves resemble closely those of disordered crystalline ω-V_2O_5 reported by Delmas et al. [2], the V_2O_5 films deposited under these conditions were observed to be amorphous in both X-ray diffraction of 1 μm thick films and in electron diffraction from 500 Å thick films deposited onto transmission electron microscopy (TEM) grids. From both Rutherford backscattering and Auger electron spectroscopy, the O/V ratio of these films is $O/V = 2.5 \pm 0.1$ Based on the cathode mass determined from a quartz crystal rate monitor and the thickness measured with a profilometer, the average density of the amorphous V_2O_5 films is about 3 g/cm^3.

The lithium manganese oxide cathodes were deposited by e-beam evaporation and by r.f. magnetron sputtering of $LiMn_2O_4$ at ambient temperatures. The evaporations were carried out in 10^{-5} torr of O_2, while for sputtering the process gas was a mixture of Ar + 10% O_2 at a total pressure of 20 mtorr. Witness films were deposited onto silicon substrates for X-ray diffraction measurements and observation of the microstructure in a scanning electron microscope. Following deposition, the evaporated films were annealed in O_2 at temperatures from 400 to 800 °C [3]. After the 800 °C anneal, the films were found to be single phase with the cubic spinel structure. The films deposited by evaporation and sputtering were X-ray amorphous before annealing.

The amorphous lithium phosphorus oxynitride electrolyte films (usually 1 μm thick) were deposited by r.f. magnetron sputtering of Li_3PO_4 in N_2. Typically, the composition of this material is $Li_{2.9}PO_{3.3}N_{0.46}$ and the conductivity 2×10^{-6} S/cm at 25 °C [1]. This electrolyte has a Li^+ transport number of unity, and, most importantly, is stable in contact with metallic Li at high-cell voltages. Lithium anode films were deposited by evaporation of lithium metal contained in a Ta crucible at a pressure of about 10^{-6} torr. Usually 3 to 5 μm thick films were deposited corresponding to at least five times more lithium than required for complete discharge of the cells. After the lithium deposition, some of the cells were transferred in Ar to another deposition system where the protective coating was applied. In other cases, the cells were connected to clip leads and placed in vacuum tight bottles with a piece of lithium foil acting as a getter.

The thin-film cells were cycled at constant current between specified voltage limits. At the end of one or both half-cycles, the voltage was held constant until the current decreased to a about 1 μA. Some of the experiments on Li–V_2O_5 cells were carried out with a home-built apparatus consisting of two Kiethley electrometers operating under computer control. Most of the d.c. measurements were carried out using a Maccor battery test system with 1 mA channels. The impedance of the cells at different potentials was measured at frequencies from 0.01 Hz to 10 MHz using the methods described elsewhere [4,5]. While the d.c. and a.c. electrical measurements were usually carried out at room temperature, several Li–V_2O_5 cells were also studied at temperatures of 0, 15, and 50 °C.

3. Results and discussion

3.1. Li–V_2O_5 cells

The Li–V_2O_5 cells were usually cycled between 3.6 and 1.5 V. Based upon the mass of the V_2O_5 films estimated from the deposition rate, within experimental error the initial discharge to 1.5 V is represented by:

$$3\,Li + V_2O_5 = Li_3V_2O_5 \qquad (1)$$

provided the cell was near equilibrium at the end of the discharge. On the subsequent charge cycle, the amount of Li extracted from the cathode is about 2.8 Li per V_2O_5 at room temperature (i.e., about 7% of the Li ions remain in the cathode after the initial discharge). This is illustrated in Fig. 3 in which the initial discharge and several subsequent cycles are shown.

With continued cycling of Li–V_2O_5 cells, the capacity decreases gradually, the rate of decrease depending on the cycling conditions including temperature. As shown in Fig. 4, the rate of capacity fading depends on the depth-of-discharge. When cycled between 3.4 and 1.5 V at room temperature, the capacity loss for this cell was about 0.1% per cycle (curves (a) and (c)), but when the voltage range was restricted between 3.1 and

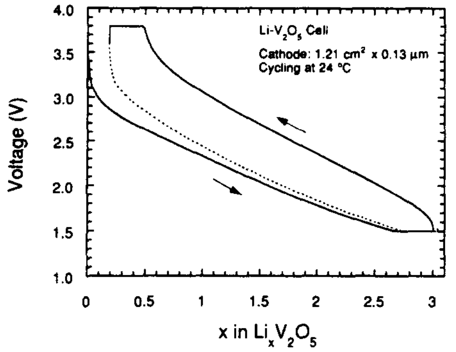

Fig. 3. Initial discharge and a first few cycles of a Li–V_2O_5 thin-film cell.

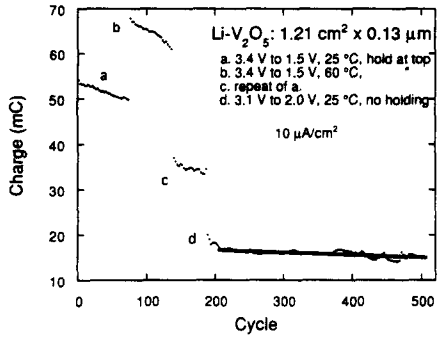

Fig. 4. Cycling behavior of the cell of Fig. 3 at a constant current of 10 μA/cm² for deep discharges at 25 and 60 °C and for a shallow discharge at 25 °C. In (a), (b), and (c), the voltage was held constant at 3.4 V until the current decreased to 1 μA. In curve (d), the current was constant at 10 μA. The solid line through the data points of (d) is the function $C = C_0(1-\delta)^n$, where C_0 is the capacity at cycle number, $n = 0$, C is the capacity after n cycles, and δ is the fraction loss per cycle.

2 V, the capacity loss was reduced to 0.034% per cycle (curve (d)). This rate of capacity fading remained the same after more than 1200 cycles.

The large initial loss in capacity and the smaller but continuous loss with cycling is caused by the entrapment of Li in the V_2O_5, possibly due to strain-induced local changes in bonding. The lithium is evidently trapped in deep potential wells since it cannot be removed by overcharging to 5 V. It is interesting to note that the rate of capacity loss increases at higher temperatures as can be seen by comparing the slope of curve (b) with those of (a) and (c). This suggests that the entrapment of Li in the cathode is a thermally activated process.

The cell resistance also increases with cycling. After a few cycles under the conditions for curve (a) in Fig. 4, the cell resistance was about 5140 Ω, but, after the 500th cycle (curve (d)), the resistance had increased to about 12 kΩ. The regions which contain the trapped, immobilized lithium evidently block the conduction paths for diffusion of the remaining mobile lithium ions. With increasing concentration and/or size of the trapping sites, the conductivity decreases.

The Li–V_2O_5 cells exhibit good shelf life. A cell that had been discharged to a resting voltage of 2.9 V was stored in a bottle with Li foil. Within experimental error, there was no change in the open-circuit voltage after 12 months of storage at room temperature.

Examples of discharge curves at different current densities and at 5 μA/cm² at different temperatures are shown in Fig. 5 and 6, respectively. In these experiments, which were performed before the extended cycle tests described above, after each discharge to 1.5 V the cell was charged to 3.6 V at 40 μA/cm², and the voltage was held at this value until the current decreased to 1 μA. The results shown in these two Figures illustrate how the useful capacity of the Li–V_2O_5 cell depended on discharge rate and temperature.

We have found that the polarization resistance evident in these data arises mainly from the slow diffusion of Li^+ in the cathode. By least-squares analysis of the impedance spectra [4,5] for several cells using the finite diffusion model of Ho et al. [6] for the cathode, the chemical diffusion coefficient of Li^+ in V_2O_5 at 25 °C is 10^{-15} to 10^{-12} cm²/s, depending on the particular cathode and the open-circuit voltage (i.e., the concentration of Li^+ in the cathode). The cell resistance decreases, in some cases by several orders of magnitude, as the lithium content increases until the cell voltage reaches about 1.5 V, then the resistance again increases

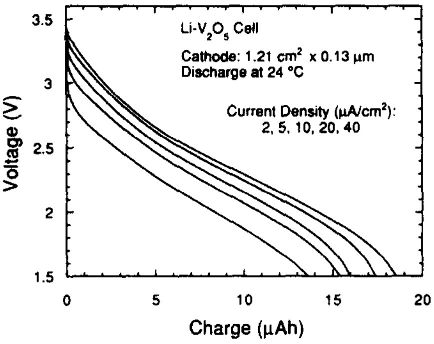

Fig. 5. Discharge curves for the cell of Fig. 3 at different current densities at 25 °C. On the charge cycle, the voltage was held constant at 3.5 V until the current decreased to 1 μA.

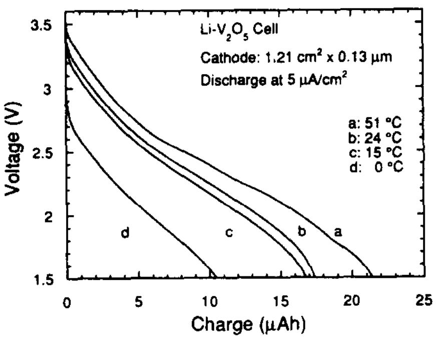

Fig. 6. Discharge curve of the cell of Fig. 3 at 5 μA/cm² for different temperatures. On the charge cycle, the voltage was held constant at 3.5 V until the current decreased to 1 μA.

as the cells are discharged below 1.5 V [5]. The impedance spectra of Li–V_2O_5 cells show [4,5] a component which is one to two orders of magnitude lower in resistance than the bulk cathode resistance at cell voltage of about 3.5 V. This extra component evidently arises from an interfacial layer that is formed between either the current collector and the cathode or between the cathode and the electrolyte. The origin of this barrier layer is presently under investigation. Because of this layer, the polarization resistance of Li–V_2O_5 cells does not simply scale with the cathode thickness since the resistance of the layer is a constant that does not change as lithium intercalates into the cathode. At voltages from about 2 to 1.5 V, the interfacial layer can contribute most of the cell resistance depending on the thickness of the cathode.

3.2. Li–$Li_xMn_2O_4$ cells

The initial charge and a few subsequent cycles of one of the Li–$Li_xMn_2O_4$ cells are shown in Fig. 7. The 0.3 μm thick cathode was deposited by e-beam evaporation and annealed in O_2 at 800 °C. At the present time, the mass of the evaporated cathodes has not been accurately measured. Based on the measured film thickness and assuming a theoretical density of 4.2 g/cm^3, the discharge capacity of 11.6 μAh between 4.5 and 3.8 V corresponds to 77 μAh/mg. We suspect, from prior experience with other types of thin films, that the density of the $LiMn_2O_4$ films is lower than theoretical so that the actual specific capacity of the cell is higher. After 300 cycles at 25 °C over the 4.5 to 3.8 V range at 20 μA/cm^2, with holding at 4.5 V on the charge cycle until $i = 1$ μA, the capacity loss per cycle in this cell was 0.006%.

The inset in Fig. 7 shows a discharge at 20 μA to 2.5 V. After the sharp transition at about 3.8 V and 11 μAh, a second plateau was observed at 2.83 V. Presumably this corresponds to the two-phase region consisting of the cubic spinel and tetragonal structures [7]. On continued discharge, a third plateau was observed at 2.5 V. The cell was evidently not stable in this region since the voltage immediately relaxed to 2.8 V on switching the discharge current to zero.

The resistance of the Li–$Li_xMn_2O_4$ cell in the 4.5 to 3.8 V region (i.e., in the single-phase spinel region) was about 285 Ω or nearly two orders of magnitude lower than that of typical Li–V_2O_5 cells with cathodes of the same area and comparable thickness. As shown in Fig. 8, this particular cell could be discharged at rates of 1 mA/cm^2 with 60% retention of useful capacity in this voltage range. These results provide further evidence that the polarization resistance of our thin-film lithium batteries is determined primarily by the Li^+ mobility in the cathode. Using the same analysis of impedance spectra described above for Li–V_2O_5 cells, the chemical diffusion coefficient of Li^+ ions in the $Li_xMn_2O_4$ cathode (4.3 V) at 25 °C is about 10^{-10} cm^2/s.

Several cells were fabricated with $LiMn_2O_4$ cathodes deposited by sputtering at ambient temperatures. Although much work to optimize the processing variables remains to be done, the preliminary results are encouraging. As for the sputter-deposited V_2O_5 cathodes, the $LiMn_2O_4$ cathodes were found to be X-ray amorphous. Some cycling results for one of the cells are shown in Fig. 9. The shape of the discharge curves is similar to that observed for the crystalline $LiMn_2O_4$ cathodes (Fig. 7), although the relative capacities associated with the 4.2 and 2.8 V plateaus differ. The polarization losses for the sputtered cathode are far larger than those for the annealed, crystalline cathode: the resistance of the charged cell of Fig. 9 was about 6000 Ω. As for the V_2O_5 cells, this cell could be cycled reversibly over a 2 V operating range.

The specific energy and power based on the cathode mass for a few of the thin-film lithium batteries we have investigated are compared in Fig. 10. The numbers near selected points are the times to discharge over the voltage range of 3.6 to 1.5 V for the Li–V_2O_5 cells, 4.5 to 3.8 V for the Li–$Li_xMn_2O_4$ cell with the annealed,

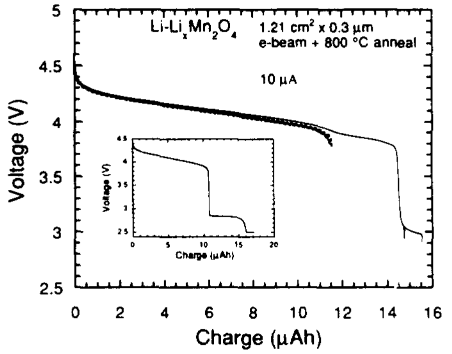

Fig. 7. The initial charge and a few cycles at 10 μA of a Li–$Li_xMn_2O_4$ cell in which the cathode was deposited by e-beam evaporation followed by annealing at 800 °C in O_2. The inset shows a discharge at 20 μA to lower voltage plateaus.

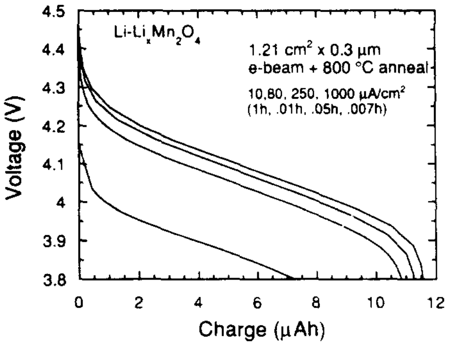

Fig. 8. Discharge curves of the Li–$Li_xMn_2O_4$ cell of Fig. 7 at 25 °C at different current densities. On each charge cycle, the voltage was held constant at 4.5 V until the current decreased to 1 μA.

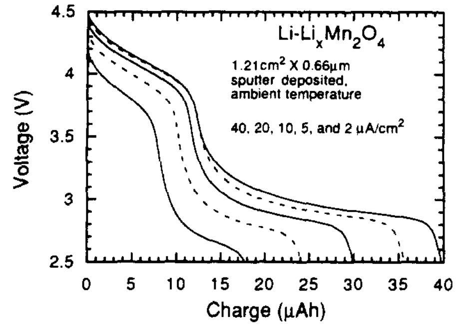

Fig. 9. Discharge curves of a Li–$Li_xMn_2O_4$ cell at 25 °C in which the cathode was deposited by sputtering at ambient temperature. On each charge cycle, the voltage was held constant at 4.5 V until the current decreased to 1 μA.

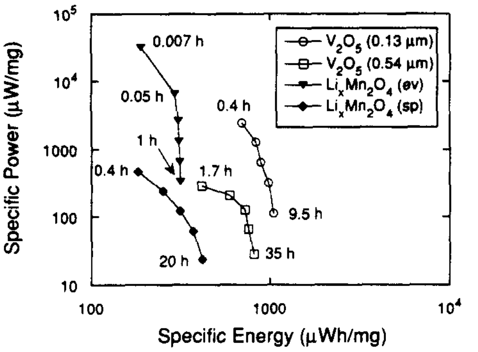

Fig. 10. Comparison of the specific power and specific energy of several thin-film lithium cells. In the legend, ev = evaporated and sp = sputtered. The numbers beside selected data points are the times to discharge over specified voltage ranges given in the text.

e-beam evaporated crystalline cathode, and 4.5 to 2 V for the Li–$Li_xMn_2O_4$ cell with the sputter deposited, amorphous cathode.

4. Conclusions and future work

The results presented in this paper show that the performance of rechargeable thin-film lithium batteries depends critically on the nature of the cathode and the methods used to deposit them as well as on the cathode geometry, operating temperature, and current density. Much of our present research efforts are directed at optimizing the current density and capacity of the V_2O_5 and $Li_xMn_2O_4$ cathodes, searching for methods to achieve acceptable performance with $LiMn_2O_4$ films at processing temperatures well below 800 °C, and exploring cells with other oxide cathodes such as $LiCoO_2$. Prototype Li–V_2O_5 and Li–$Li_xMn_2O_4$ batteries for several types of new, potentially commercial electronic devices are under investigation.

Acknowledgements

The authors thank Mr Chris Luck for fabricating many of the cells discussed in this work and Dr Matthew Chisholm for performing the electron diffraction measurements on the thin V_2O_5 cathode. This research was sponsored by the US Department of Energy, Division of Materials Sciences, Office of Transportation Technologies, Division of Chemical Sciences, and Office of Energy Research Technology Transfer Program under contract DE-AC05-84OR21400 with Martin Marietta Energy Systems, Inc.

References

[1] J.B. Bates, N.J. Dudney, G.R. Gruzalski, R.A. Zhur, A. Choudhury, C.F. Luck and J.D. Roberts, *J. Power Sources, 43/44* (1993) 103.
[2] C. Delmas, S. Brethes and M. Menetrier, *J. Power Sources, 34* (1991) 113.
[3] F.K. Shokoohi, J.M. Tarascon and B.J. Wilkens, *Appl. Phys. Lett., 59* (1991) 1260.
[4] J.B. Bates, G.R. Gruzalski, N.J. Dudney, C.F. Luck and X. Yu, *Solid State Ionics, 70/71* (1994) 619.
[5] J.B. Bates, G.R. Gruzalski, N.J. Dudney, C.F. Luck and X. Yu, *Proc. Symp. Science of Advanced Batteries, 8–9 Nov. 1993, Cleveland, OH, USA*, The Electrochemical Society, Pennington, NJ, USA, 1994, in press.
[6] C. Ho, I.D. Raistrick and R.A. Huggins, *J. Electrochem. Soc., 127* (1980) 343.
[7] T. Ohzuku, M. Kitagawa and T. Hirai, *J. Electrochem. Soc., 137* (1990) 769.